

Identification of the relationships between noncontact capacitive sensing signals and continuous grasp forces: Preliminary study

Enhao Zheng¹, Qining Wang^{2,4} and Hong Qiao^{1,3}

Abstract—This study explores the relationships between noncontact capacitive sensing signals and continuous grasp forces. It is a crucial step towards the volitional control of robotic systems based on the noncontact sensing approach. We firstly designed a measurement system including the capacitive sensing front-ends, the grasp force sensor, the signal sampling circuits and the graphic user interface. The capacitive sensing front-end was specifically designed for human forearm signal sampling, which was worn outside of the clothes. After implementation of the system, we carried out experiments on five healthy subjects, and the sensing bands were customized with their arm shapes. The grasp force and the capacitance signals were record simultaneously when the subjects gradually increased the force according to instruction. Linear regression and quadratic regression were used to evaluate the regulated signals. For each subject, at least one channel of capacitance signals were linear correlated to the normalized grasp force with $R^2 \geq 0.85$. We found there was inter-subject similarity on the capacitance-force relationships. Cross validation on grasp force estimation with capacitance signals were also carried out, and the average relative estimation error was about 18%. The results proved the feasibility of the noncontact capacitive sensing method for human joint force estimation.

I. INTRODUCTION

Human machine interfaces (HMIs) based on muscle signals are attracting more and more attentions in robotic research field. One critical issue of HMIs is bridging the gap between human motion intentions and the robotic control systems. In human motions, the muscles behave as the actuators of the sensory-motor system, the contractions of which contains abundant motion intent information [1]. Human regulate muscle contraction forces in unpredicted environment to stabilize the motion tasks [2], [3]. Perceiving the muscle force information of human motion plays an important role in robotic control [4]–[6].

Among the existing technologies in muscle signal re-coding, sEMG-based sensing method is the most widely

used. Due to its noninvasiveness to human body and the physical significance of the signals, many studies were conducted in mapping the sEMG signals to the specific joint force information [7]–[12]. Although progressive results were obtained, claimed by many studies, the limitations of sEMG sensing methods are obvious and also problematic in practical applications [13]. The sweats on the skin seriously decrease the sEMG signal quality, due to the contacting of the metal electrodes on human skin. To compensate the limitations in the sensing principle, attempts are being made on other signal sources [13], [14]. For example, the ultrasound imaging methods provided a promising solution for HMIs [13]. However, in measuring, the probe of the ultrasound imaging system was also placed on human skin, and ultrasound gel was needed to insure the signal quality [15]. Above all, accurate and stable extraction of human intent information is still a challenging task.

In our previous works, we proposed a noncontact capacitive sensing strategy for human motion intent recognition [16]–[18]. In this method, the metal electrodes were fixed on the inner surface of the sensing front-ends, and they were insulated from human skin by a layer of cloth. When there were muscle shape changes brought by human motions, the gap between the human body and the electrode would change, which accordingly changed the capacitance signals. Our previous studies proved the effectiveness of the new method for locomotion mode recognition [16], [17] and gait phase estimation [18]. The capacitive sensing suggest a promising solution for human intent recognition. However, the previous studies only involved indirect motion mode or state recognition, in which the tasks were predefined motion patterns. The statistical characteristics of the capacitance signals were extracted from the training data by algorithms. The direct relationship between capacitance signals and joint forces were unknown, which was also important for intent-based robotic control [10].

The contributions of this study are twofold. Firstly, we addressed the problems of relating the capacitance signals with forearm joint force information. We designed a measurement system that can simultaneously measure the capacitance signals and the grasp forces in continuous tasks. Secondly, we proved the feasibility of using noncontact capacitive sensing method for joint force estimation. Regression methods were investigated and evaluated on multiple subjects. It not only extent the works of capacitive sensing based human intent recognition, but also provided a promising alternative solution to the existing muscle signal sensing methods.

*This work was supported by the National Natural Science Foundation of China (No. 61703400, No. 91648207 and No. 61627808), and Beijing Natural Science Foundation (No. L172052).

¹Enhao Zheng is with The State Key Laboratory of Management and Control for Complex Systems, Institute of Automation, Chinese Academy of Sciences, No. 95 of Zhongguancun East Road, Beijing, China. enhao.zheng@ia.ac.cn

^{2,4}Qining Wang is with The Robotics Research Group, College of Engineering, Peking University, Beijing 100871, China. He is also with The Beijing Innovation Center for Engineering Science and Advanced Technology (BIC-ESAT), Peking University, Beijing, China. qiningwang@pku.edu.cn

^{1,3}Hong Qiao is with The State Key Laboratory of Management and Control for Complex Systems, Institute of Automation, Chinese Academy of Sciences, No. 95 of Zhongguancun East Road, Beijing, China. She is also with the University of Chinese Academy of Sciences, Beijing, 100049, China. hong.qiao@ia.ac.cn

II. METHODS

A. Measurement system

The measurement system comprised the capacitive sensing front-ends, the force sensor and the signal sampling circuits (upper half of Fig. 1). The sensing front-ends were designed to be dressed on human forearm. It was a C-shaped band with the gap located at the medial side of the forearm (bottom right of Fig. 1). Six copper films were fixed on the inner surface (the side of human body), which served as the electrodes of the capacitive sensing system. As the sensing band was dressed outside of the cloth, each copper film formed a plate capacitor with human body and the cloth between them. When there were limb deformations caused by muscle contractions, the distance between the two equivalent electrodes (copper film and human body) would change and it further lead to the capacitance value changes. More detailed descriptions of the sensing principles could be found in [16]. The sensing band was made of thermoplastic material, and it was customized based on the limb shape of the subject. A bandage was fabricated on the gap of the sensing band to adjust the tightness. In order to record the capacitance values, the sampling circuit was designed to measure the charge-and-recharge cycle time of the capacitors. A reference capacitor was used for converting the cycle time to actual capacitance values. In order to measure the grasp force, a force sensor was implemented on the measurement system. The forces were measured through the strain gauges placed on the middle part of the sensor (bottom left of Fig. 1). The measuring range of the force sensor was 0-800 N. As there was a resistance bridge circuit inside the sensor, it required a direct current (DC) excitation voltage of 10 V. The output signal was voltage and the resolution was 2.068 mV/V. The voltage was linearly amplified to the range of 0-3.3 V by the specifically designed sampling circuit, then it was digitalized by a 12-bit analog-to-digital converter (ADC). The data of capacitance signals and grasp force were packaged by the designed control circuit in each 10 ms. We designed a GUI to regulate the signals and conduct the experiment.

B. Experiment protocol

In this study, five male healthy subjects were employed. All of them were provided written and informed consent. They had an average age of 23.6 ± 3.1 years, an average height of 177.2 ± 7.2 cm, and an average weight of 74.6 ± 10.7 kg. We measured signals from their right forearms. The average forearm length of the subjects was 23.6 ± 1.8 cm, which was the length between the styliion radiale and the radiale (elbow joint) with the arm sagging naturally. The average forearm circumference across the subjects was 25.0 ± 1.4 cm which was measured from the most prominent part of the forearm. Although the subjects had similar forearm length and circumference, the individual difference of the arm shape could influence the system setups. We therefore customized the sensing band for each subject before the experiment. The length of the sensing band was designed

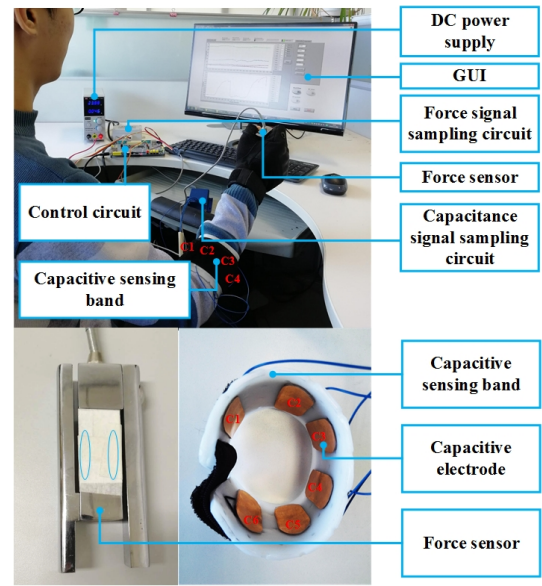


Fig. 1. Experimental setups of the study (top half of the figure). The force sensor (bottom left) and the capacitive sensing band (bottom right). In GUI, the raw capacitance signals and the force signals were presented in real time. During the measuring, the capacitive sensing band and the force sensor was placed on the right arm. The sensing band was dressed outside of the clothes of the subjects. The signal channels were distributed as the red font C_x , $x = 1, 2, \dots, 6$. The DC power supply was used to provide voltage to the force signal sampling circuit. The control circuit synchronized the signals from the signal sampling circuits and transmitted them to the computer. The force sensor record the grasp force by the strain gauges placed in the middle of the mechanical structure, as shown in the blue circles in the bottom left of the figure.

based on the forearm circumference. We set a 2-cm gap on the medial side of the forearm for bandage fabrication. The width of the band was 7 cm. During the experiments, the subjects wore their own sensing bands outside of the clothes and adjusted the bandage based on their own feelings. The setups of the experiment was shown in Fig. 1. After the familiarization procedure of several minutes, the subjects were asked to gradually increase their grasp force to his maximum contraction within 5 seconds and relaxed. The procedure repeated ten times (trials) with the rest of 5 to 10 seconds between two successive contractions. In GUI, the capacitance signals and the force sensor signals were shown in separate panels for visual feedback to assist them in controlling the contraction speed. The experiment procedures were approved by the Institutional Review Board of CASIA.

C. Data processing

All signals were sampled at 100 Hz. The capacitance signals went through a 4-th order Butterworth low-band-pass filter with the cut-off frequency of 5 Hz. For the force signals, we firstly designed a five-point median filter to remove the random noise. Then a 1st-order lag filter was implemented to further smooth the force signals. The filtered force signals were normalized from 0% MVC to 100% MVC for each subject. Filtered signals were shown as Fig. 2. With initial trials, we found the subject difficult to control the grasp force decreasing speed, which was also reported by other

related studies [19]. We therefore extracted the signals of force increasing period, i.e. the period from 0% MVC to 100% MVC.

D. Evaluation method

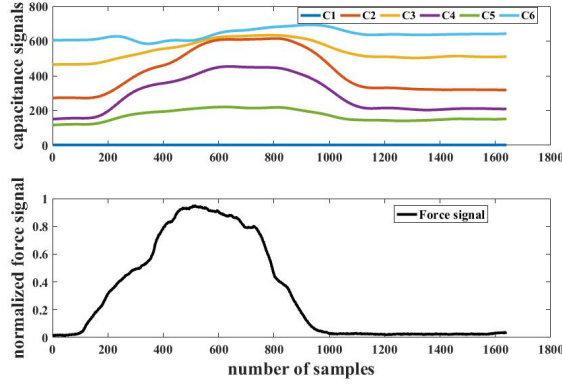


Fig. 2. The filtered capacitance signals (upper figure) and the normalized force signal (bottom figure) of one trial. The data were collected from the first trial of subject2.

We used linear regression and quadratic regression to fit the capacitance signals with the normalized grasp force signals. To evaluate the performances, square of the correlation coefficient (R^2) and relative root mean square errors (RRMSE) were calculated for each subject. The RRMSE was expressed as:

$$RRMSE = \sqrt{\frac{\sum_i^M (\hat{Y}(i) - Y(i))^2}{\sum_i^M Y(i)^2}}, \quad (1)$$

where $\hat{Y}(i)$ was the i -th calculated data point by the regression model, $Y(i)$ was the i -th actual data point, and M was the number of points in total. The value changed between 0 and 1, with smaller values indicating better results.

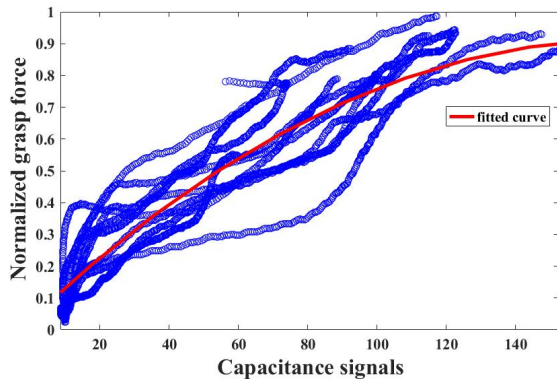


Fig. 3. The phase plot of the capacitance signals and the normalized force signal. The horizontal axis was the capacitance signals, and each sample was denoted as the blue circles. The red line was the fitted curve by quadratic regression. The data were collected from the 3rd channel of the capacitive sensing system of subject2.

TABLE I

REGRESSION RESULTS OF FIVE SUBJECTS WITH LINEAR FITTING.

Subject number	Channel number					
	C1	C2	C3	C4	C5	C6
Subject1	0.01	0.16	0.89	0.00	0.68	0.79
	0.55	0.51	0.19	0.55	0.31	0.26
Subject2	0.01	0.90	0.84	0.88	0.85	0.05
	0.49	0.15	0.19	0.17	0.19	0.48
Subject3	0.00	0.59	0.91	0.24	0.59	0.15
	0.56	0.36	0.17	0.49	0.36	0.52
Subject4	0.00	0.00	0.85	0.00	0.01	0.45
	0.50	0.50	0.19	0.50	0.50	0.37
Subject5	0.00	0.87	0.00	0.47	0.04	0.08
	0.46	0.17	0.46	0.34	0.45	0.45

TABLE II

REGRESSION RESULTS OF FIVE SUBJECTS WITH QUADRATIC FITTING.

Subject number	Channel number					
	C1	C2	C3	C4	C5	C6
Subject1	0.04	0.18	0.89	0.31	0.72	0.79
	0.54	0.50	0.18	0.46	0.29	0.25
Subject2	0.02	0.91	0.86	0.88	0.85	0.16
	0.48	0.15	0.18	0.17	0.19	0.45
Subject3	0.01	0.63	0.91	0.36	0.62	0.28
	0.56	0.34	0.17	0.45	0.35	0.48
Subject4	0.01	0.48	0.85	0.15	0.08	0.49
	0.50	0.36	0.19	0.46	0.48	0.36
Subject5	0.01	0.88	0.36	0.53	0.77	0.28
	0.46	0.16	0.37	0.32	0.22	0.39

III. RESULTS

We evaluated the performance by linear regression (Table I) and quadratic regression (Table II) for all the signal channel (C1 to C6 in the tables) and the five subjects. The data of all the trials were used for curve fitting. One typical fitting result was shown in Fig. 3. We could see from the tables that different signal channels produced various regression results. For subject1, C3 produced the best results (highest R^2 s and lowest RRMSE), for both regression methods. While the best channels for subject2 and subject3 were C2 and C3, respectively. Among the subjects, S2 produced better results than the others. The R^2 s of four channels (C2, C3, C4 and C5) were larger than 0.84. For all the subjects, C1 performed the worst results ($R^2 = 0.1$). We compared the results of the two regression methods, there were large differences for most of the signal channels. However, for the best channel of each subject (C3 for subject1, subject3 and subject4, C2 for subject2 and subject5), the values of R^2 and RRMSE were similar. For RRMSE, the lowest values were 0.19, 0.15, 0.17, 0.19 and 0.17 for the best channels of five subjects respectively.

We also investigated the performance with N-fold leave-one-out-cross validation (LOOCV). In LOOCV, the data of one fold (trial) served for testing, while the rest data were training set. The training data were fitted with the regression method (linear and quadratic), the fitted curve was tested on the testing data set. The procedure was repeated for N

times until all the data were used. In this study, N was set to be ten. The best channels of the subjects were selected for LOOCV analysis. With linear regression method, the average R^2 across five subjects was 0.86 ± 0.03 , and the average RRMSE was 0.18 ± 0.02 . The average R^2 and RRMSE across five subjects with quadratic regression was the same as that of linear regression.

IV. DISCUSSION AND CONCLUSION

In this study, we investigated the relationships between the noncontact capacitive sensing signals and the grasp forces simultaneously. Results can be summarized as follows. Firstly, for each subject, there were at least one signal channel that was linearly correlated with the grasp forces ($R^2 \geq 0.85$) when the subject continuously increased his forearm muscle contractions. Secondly, there were obvious individual differences of the overall regression results (see Table I and Table II). However, the best channels selected for the subjects (with the highest R^2 and lowest RRMSE) were concentrated on channel2 and channel3, which were distributed on the brachioradialis and extensor carpus radialis. Thirdly, we evaluated the feasibility of continuous grasp force estimation by capacitance signals. With off-line LOOCV, the tested RRMSE and R^2 were similar to that of the whole data used.

The novelties of the results are two fold. First, as an alternative solution to the muscle signal sensing, capacitive sensing approach could measure muscle signals with a noncontact way. This study extent our previous works by proving the feasibility of the sensing approach on continuous voluntary muscle contraction estimation. Compared with the existing sEMG-based studies [7]–[10], the noncontact capacitive sensing method produced similar regression results. The yielded R^2 with sEMG signals on wrist joint torque estimation was about 0.9, being the same level as our study (≥ 0.85). Second, the inter-subject similarity on signal channels could benefit future applications on intuitive control of robotic devices. It offered an opportunity to accelerate the configuration procedure for new individuals.

On the other side, this is a preliminary study and the results are limited in the following aspects. In this study, only five healthy subjects were employed and only off-line estimation task was evaluated. The performances of the sensing system with disturbances including the re-wearing procedure, the inter-day use and long-term monitoring remain to be addressed. The regression models used in this study were simple. The estimation error rate (about 18% of RRMSE with LOOCV) was also a little higher than the sEMG-based studies (error rate $< 10\%$) [7]–[10].

be explored. What's more, on-line estimation method will

Nevertheless, the results were still promising and the direction was worth being exploited. In the future, more extensive experiments on more subjects will be conducted. In addition to continuous grasp forces, more complicated tasks with multiple joint degree of freedoms (DoFs) will be addressed. More regression models will be designed to get more accurate joint force estimation. In addition to joint forces, the relationships of capacitance signals with other joint information (such as joint stiffness) will also

be designed for robotic device control. We envisioned that in future application scenarios, the noncontact capacitive sensing approach can be used with other sensors and provide human motion intent recognition for robotic control.

REFERENCES

- [1] S. H. Scott, Optimal feedback control and the neural basis of volitional motor control, *Nat. Rev. Neurosci.*, vol. 5, no. 7, pp. 532-546, 2004.
- [2] E. Burdet, R. Osu, D. W. Franklin, T. E. Milner, and M. Kawato, The central nervous system stabilizes unstable dynamics by learning optimal impedance, *Nature*, vol. 414, no. 6862, pp. 446-449, 2001.
- [3] D. W. Franklin, E. Burdet, K. P. Tee, R. Osu, C. M. Chew, T. E. Milner, and M. Kawato, CNS learns stable, accurate, and efficient movements using a simple algorithm, *J. Neurosci.*, vol. 28, no. 44, pp. 11165-11173, 2008.
- [4] D. Farina, N. Jiang, H. Rehbaum, A. Holobar, B. Graimann, H. Dietl and O. C. Aszmann, The extraction of neural information from the surface EMG for the control of upper-limb prostheses: emerging avenues and challenges. *IEEE Trans. Neural. Sys. Rehab. Eng.*, vol. 22, no. 4, pp. 797-809, 2014.
- [5] C. Fleischer and G. Hommel, A human-exoskeleton interface utilizing electromyography, *IEEE Trans. Robot.*, vol. 24, no. 4, pp. 872-882, 2008.
- [6] M. Howard, D. J. Braun and S. Vijayakumar, Transferring human impedance behavior to heterogeneous variable impedance actuators, *IEEE Trans. Robot.*, vol. 29, no. 4, pp. 847-862, 2013.
- [7] S. N. Sidek and A. J. Haja Mohideen, Mapping of EMG signal to hand grip force at varying wrist angles, in *Proc. of 2012 IEEE-EMBS Conference on Biomedical Engineering and Sciences*, Langkawi, 2012, pp. 648-653.
- [8] E. N. Kamavuako, E. J. Scheme, and K. B. Englehart, Wrist torque estimation during simultaneous and continuously changing movements: surface vs. untargeted intramuscular EMG, *J. Neurophysiol.*, vol. 109, pp. 2658-2665, 2013.
- [9] Z. Yang, Y. Chen, Z. Tang, and J. Wang, Surface EMG based hand grip force predictions using gene expression programming, *Neurocomputing*, vol. 207, pp. 568-579, 2016.
- [10] M. Kim, J. Lee and K. Kim, Tele-operation system with reliable grasping force estimation to compensate for the time-varying sEMG feature, in *Proc. of 2016 IEEE International Conference on Robotics and Automation (ICRA)*, Stockholm, 2016, pp. 5561-5567.
- [11] M. Howard, D. J. Braun and S. Vijayakumar, Transferring human impedance behavior to heterogeneous variable impedance actuators, *IEEE Trans. Robot.*, vol. 29, no. 4, pp. 847-862, 2013.
- [12] F. Lunardini, C. Casellato, A. d'Avella, T. D. Sanger and A. Pedrocchi, Robustness and reliability of synergy-based myoelectric control of a multiple degree of freedom robotic Arm, *IEEE Trans. Neur. Sys. Rehab. Eng.*, vol. 24, no. 9, pp. 940-950, 2016.
- [13] C. Castellini, State of the art and perspectives of ultrasound imaging as a human-machine interface, in *Neuro-Robotics From Brain Machine Interfaces to Rehabilitation Robotics*, Netherlands: Springer, 2014, pp. 37-58.
- [14] A. Radmand, E. Scheme and K. Englehart, High-density force myography: A possible alternative for upper-limb prosthetic control, *J. Rehabil. Res. Dev.*, vol. 53, no. 4, 2016.
- [15] G. Zhou, Human motion analysis with sonomyography, Ph.D. Thesis, The Hong Kong Polytechnic Univ., Hong Kong, China, 2015.
- [16] E. Zheng, L. Wang, K. Wei, and Q. Wang, A noncontact capacitive sensing system for recognizing locomotion modes of transtibial amputees, *IEEE Trans. Biomed. Eng.*, vol. 61, pp. 2911-2920, 2014.
- [17] E. Zheng, and Q. Wang, Noncontact capacitive sensing-based locomotion transition recognition for amputees with robotic transtibial prostheses. *IEEE Trans. Neural Syst. Rehabil. Eng.*, vol. 25, no. 2, pp. 161-170, 2017.
- [18] E. Zheng, S. Manca, T. Yan, A. Parri, N. Vitiello, and Q. Wang, Gait phase estimation based on noncontact capacitive sensing and adaptive oscillators. *IEEE Trans. Biomed. Eng.*, vol. 64, no. 10, pp. 2419-2430, 2017.
- [19] J. Shi, Y. P. Zheng, Q. H. Huang and X. Chen, Continuous Monitoring of Sonomyography, Electromyography and Torque Generated by Normal Upper Arm Muscles During Isometric Contraction: Sonomyography Assessment for Arm Muscles, *IEEE Trans. Biomed. Eng.*, vol. 55, no. 3, pp. 1191-1198, 2008.